Available online at www.sciencedirect.com
SCIENCE DIRECT®
Solar Energy 80 (2006) 535–544
SOLAR ENERGY
www.elsevier.com/locate/solener

Critical evaluation of solar chimney power plant performance

J.P. Pretorius *, D.G. Kröger

Department of Mechanical Engineering, University of Stellenbosch, Private Bag X1, Matieland 7602, South Africa

Received 18 October 2004; received in revised form 6 April 2005; accepted 8 April 2005
Available online 11 May 2005

Communicated by: Associate Editor Manuel Romero-Alvarez

Abstract

This paper evaluates the influence of a recently developed convective heat transfer equation, more accurate turbine inlet loss coefficient, quality collector roof glass and various types of soil on the performance of a large scale solar chimney power plant. Results indicate that the new heat transfer equation reduces plant power output considerably. The effect of a more accurate turbine inlet loss coefficient is insignificant, while utilizing better quality glass enhances plant power production. Models employing Limestone and Sandstone soil produce virtually similar results to a Granite-based model. The plant collector height is found to differ from previously obtained optimal values.

Keywords: Solar chimney; Solar energy; Solar power; Solar tower; Upwind; Power plant; Renewable energy

1. Introduction

A solar chimney power plant consists of a circular transparent canopy or roof raised a certain height from the ground, with a chimney or circular tower at its centre (Fig. 1). The chimney houses one or more turbo-generators located at its base. Radiation from the sun penetrates the collector roof and strikes the ground surface beneath it. The heated ground in turn heats the adjacent air. The warm air underneath the collector flows towards and up into the central chimney to drive the turbo-generators.

Haaf et al. (1983), Haaf (1984) and Schlaich (1994) described the operation and presented results for a prototype solar chimney power plant built in Manzanares, Spain in 1982. Studies by Yan et al. (1991) and Padki and Sherif (1999) conducted some of the earliest work on the thermo-fluid analysis of a solar chimney power plant. Pasumarthi and Sherif (1998a) developed an approximate mathematical model for a solar chimney power plant and in a following publication (Pasumarthi and Sherif, 1998b) verified the model against experimental test results from the prototype solar chimney plant at Manzanares. Early comprehensive published analyses of solar chimney power plant performance were conducted by Kröger and Buys (2001) and Gannon and Von Backström (2002), while Gannon and Von Backström (2003) also studied the performance of turbines to be employed in solar chimney power plants. Bernardes et al. (2003) developed an analytical and numerical model for a solar chimney power plant, comparing simulation predictions to experimental results from the pilot plant at Manzanares. Pretorius et al. (2004) also developed a numerical model simulating the performance of a large-scale reference solar chimney power plant, indicating that greater power production is possible by optimizing the collector roof shape and height. The present study extends this

* Corresponding author. Fax: +27 21 808 4958.
E-mail address: jpp@sun.ac.za (J.P. Pretorius).

0038-092X/$ - see front matter © 2005 Elsevier Ltd. All rights reserved.
doi:10.1016/j.solener.2005.04.001

Nomenclature

b	exponent or coefficient [W $s^{1/2}$/K m^2]
C	coefficient
c	specific heat capacity [J/kg K]
d	diameter [m]
f	friction factor
g	gravitational acceleration
H	height [m]
h	convective heat transfer coefficient [W/m^2 K]
K	loss coefficient
k	thermal conductivity [W/m K]
n	refractive index or number
P	pitch [m]
p	pressure [N/m^2]
Pr	Prandtl number
Re	Reynolds number
r	radius [m]
t	thickness [m]
T	temperature [K] or [°C]
v	velocity [m/s]

Greek symbols

α	absorptance
Δ	differential
ϵ	emittance
ε	roughness [m]
μ	dynamic viscosity [kg/ms]
ρ	density [kg/m^3]

Subscripts

a	ambient air
bw	bracing wheel
c	chimney
D	drag
e	extinction
g	ground
gh	ground to air under collector roof
h	air under collector roof or hydraulic
i	inlet
m	mean
p	pressure or penetration
r	roof or radial
ra	collector roof to ambient air
rh	collector roof to air under collector roof
s	support
t	tangential
tg	turbo-generator
turb	turbine
turb,i	turbine inlet
w	wind

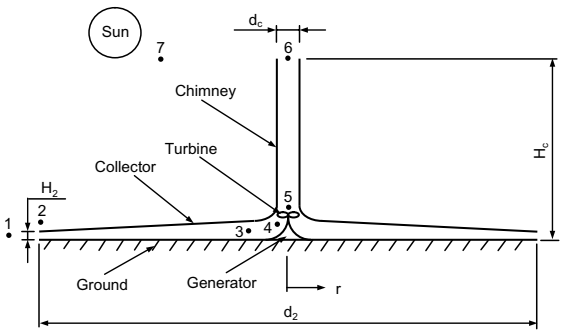

Fig. 1. Schematic illustration of a solar chimney power plant.

analysis by employing the computational model developed by Pretorius et al. (2004) to evaluate the influence of various equations and other variables on the performance of a solar chimney power plant.

2. Convective heat transfer equation

2.1. Convection to ambient

Previous studies (Hedderwick, 2001; Kröger and Buys, 2001; Pretorius et al., 2004) employed the following very approximate equation by McAdams (1954) in evaluating the convective heat transfer coefficient from the solar collector roof to the ambient air

$$h_{ra} = 5.7 + 3.8v_w \tag{1}$$

Work by Kröger and Burger (2004) has led to the development of an improved correlation for the local convective heat transfer coefficient from a horizontal surface exposed to the natural environment. More recent work by Burger (2004) led to the development of an improved version of this correlation, represented by Eq. (2). The correlation is applicable to heated horizontal surfaces facing up or cooled horizontal surfaces facing down. The experimental work by Burger (2004) (for determination of Eq. (2)) considers an energy balance which evaluates the various convective and radiative heat fluxes onto/from a horizontal flat plate exposed to the natural environment. It should be noted that the radiative heat flux from the plate to the environment is based on the sky emittance according to Berdahl and Fromberg (1982). During times when the collector roof temperature (T_r) exceeds the ambient temperature (T_a), the roof is approximated as a heated horizontal surface facing up. The top and bottom collector roof surfaces are assumed to be smooth, as indicated in Appendix A of this paper.

Henceforth, Eq. (2) replaces Eq. (1) for the evaluation of h_{ra} in the computational model during such periods. During periods when $T_a > T_r$ (and the roof is approximated as a cooled horizontal surface facing up), h_{ra} is assumed to be negligible in the absence of winds.

$$h = \frac{0.2106 + 0.0026 v_w (\rho T_m / \mu g \Delta T)^{1/3}}{(\mu T_m / g \Delta T c_p k^2 \rho^2)^{1/3}} \quad (2)$$

During the experiments conducted to develop the mixed convection heat transfer Eq. (2), the ambient air temperature was measured at 1 m above the surface. It should be noted that during operation of the actual solar chimney power plant, the hot collector roof will cause the ambient air adjacent to the roof to rise. The rising air together with entrainment thereof by the air exiting the chimney will result in a radial airflow over the roof from the collector perimeter inwards toward the chimney. Secondary flow patterns due to instabilities of the heated air above the collector may also occur. These factors may introduce additional complications in the prediction of the heat transfer from the collector roof.

2.2. Convection from roof to collector air

During periods when the collector roof temperature (T_r) is greater than the collector air temperature (T), the roof is approximated as a heated horizontal surface facing down, while when $T > T_r$ the roof is seen as a cooled flat surface facing down. By approximating the flow in the collector as flow between parallel plates, the forced convection heat transfer coefficient (this equation does not consider natural convection effects) from the collector roof to the air in the collector (h_{rh}) may be determined using Gnielinski's equation for turbulent flow (with $d_h = 2H$ the hydraulic diameter)

$$h = \frac{(f/8)(Re - 1000)Pr}{1 + 12.7(f/8)^{1/2}(Pr^{2/3} - 1)} \left(\frac{k}{d_h}\right) \quad (3)$$

Pretorius et al. (2004) employed Eq. (3) for the evaluation of h_{rh} for $T_r > T$ and $T > T_r$. Both Eqs. (2) and (3) are now applicable when calculating h_{rh} when $T > T_r$. It should be made clear that Eq. (2) considers natural and forced convection effects, while Eq. (3) only regards forced convection effects. However, Eq. (3) does consider the effects of surface roughness. It is assumed that the local heat transfer mechanism (natural convection thermals or stable layer "swept away" by forced convection) will dominate the local heat transfer rate. Therefore, with $T > T_r$ the improved numerical model employs the higher of the h_{rh} values calculated by Eqs. (2) and (3), while still only using Eq. (3) when $T_r > T$.

2.3. Convection from ground to collector air

When the ground surface temperature (T_g) exceeds the collector air temperature (T), the ground is effectively a heated horizontal surface facing up. Conversely, the ground surface is approximated as a cooled flat surface facing up during times when $T > T_g$. The ground surface is assumed to have a certain roughness, as specified in Appendix A of this paper. Analogous to the evaluation of h_{rh}, Pretorius et al. (2004) determined the convective heat transfer coefficient from the ground to the collector air (h_{gh}) by using only Eq. (3) for $T_g > T$ or $T > T_g$. However, the improved numerical model applies a similar strategy for evaluating h_{gh} and h_{rh}, due to the similar heat transfer mechanisms at play in both cases. Once again it is assumed that the local heat transfer mechanism (natural convection thermals or stable layer "swept away" by forced convection) will dominate the local heat transfer rate. Consequently, with $T_g > T$ the greater of the h_{gh} coefficients determined by Eq. (2) and (3) are employed.

It is important to note that for both the convective heat transfer from the roof and ground to the collector air, Eq. (3) is usually only applicable over a small part of the collector for a limited period (see Fig. 3). This therefore illustrates the major impact that Eq. (2) has in predicting the convective collector heat fluxes and ultimately in determining the overall plant performance.

2.4. Simulation and results

Comparative computer simulations were conducted for a reference solar chimney power plant ("Configuration A" plant with specifications listed in Appendix A of this paper), with one model employing the original strategy and equations for the calculation of the various convective heat transfer coefficients, while the other includes the recently developed correlation as mentioned above. Simulations were repeated to allow ground energy flows to reach a quasi-steady-state.

A comparison between the maximum electrical plant output for 21 June and 21 December is illustrated in Fig. 2. Table 1 compares the annual power output of the two simulation models. From Fig. 2 it is evident that the maximum output of the solar chimney power plant is somewhat reduced when employing the improved convective heat transfer correlation. Table 1 confirms a reduced output, showing a significant drop in annual power generation of 11.7%. Fig. 3 sheds some light on this considerable power reduction by presenting the values of various convective heat transfer coefficients at specific collector radii, at 13:00 on 21 December.

It is clear that the original (Eq. (3)) value for h_{gh} (from model incorporating previous equations) is almost equivalent to the new (Eqs. (2) or (3)) h_{gh} value (from model incorporating recently developed equation) when considering the outer third of the collector. At smaller radii, the original h_{gh} value decreases from approximately 19 W/m^2 K to 10 W/m^2 K while the new heat transfer coefficient remains virtually constant at just

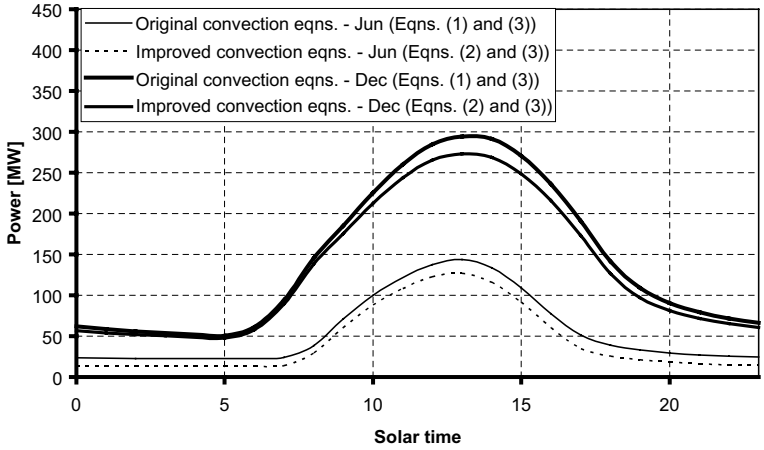

Fig. 2. Effect of the inclusion of an improved convective heat transfer equation.

Table 1
Annual power output comparison, illustrating the effect of the inclusion of a recently developed convective heat transfer correlation

Plant configuration	Annual power output [GWh]
Configuration A model, incorporating original heat transfer equations	879.5
Configuration A model, incorporating improved convective heat transfer correlation	776.4

above 19 W/m^2 K as the airflow approaches the chimney inlet. The higher convection coefficient facilitates more energy to be extracted from the ground into the air, resulting in a lower ground surface temperature. The original and new h_{rh} values start out equal at 6.5 W/m^2 K near the collector perimeter, with the new coefficient increasing significantly to 18.5 W/m^2 K while the original h_{rh} value decreases somewhat to approximately 4 W/m^2 K. Due to the fact that $T > T_r$ at 13:00, energy is transferred from the flowing collector air to the collector roof. The considerably enhanced (new) convective heat transfer coefficient results in a significantly greater heat transfer from the collector air to the roof than predicted before. From Fig. 3 it is also evident that the original h_{ra} value stays constant at 5.7 W/m^2 K while the new value for h_{ra} is slightly higher, almost throughout.

With increased heat transfer from the ground to the roof, as well as a somewhat higher h_{ra} value, more energy is lost through the collector roof to the environment than was previously predicted, resulting in a power output reduction.

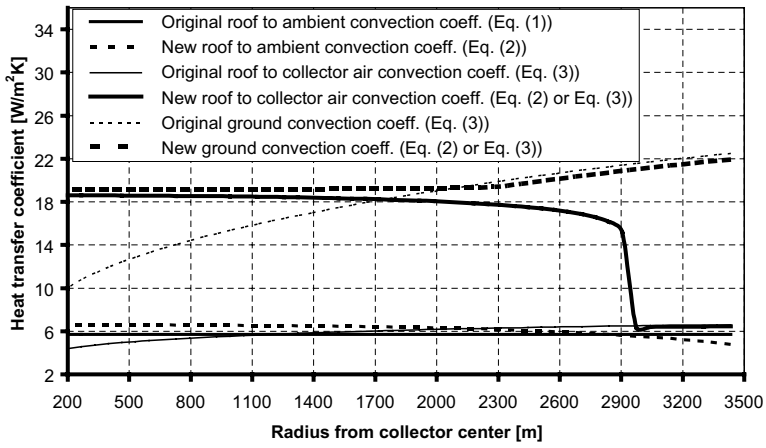

Fig. 3. Comparison between the original and new convective heat transfer coefficients.

3. Turbine inlet loss coefficient

The collector air flowing into the turbine at the base of the chimney experiences a pressure drop due to the decreasing flow area. This pressure drop is based on a turbine inlet loss coefficient, $K_{turb,i}$. The previously used $K_{turb,i}$ value of 0.25, employed by Hedderwick (2001), Kröger and Buys (2001) and Pretorius et al. (2004) was originally selected as a conservative first approximation value. After consulting Von Backström et al. (2003) it was decided to introduce a more realistic value of $K_{turb,i} = 0.14$ into the plant specifications.

3.1. Simulation and results

The "Configuration B" solar chimney power plant model is defined as equivalent to the "Configuration A" model, however incorporating the new convective heat transfer correlation (Eq. (2)) and the above-mentioned more realistic turbine inlet loss coefficient. A simulation was run for the "Configuration B" model and compared to the results of the "Configuration A" model that incorporates the improved heat transfer relation. Hereby the effect of the inclusion of the new $K_{turb,i}$ value is investigated.

Fig. 4 compares the maximum electrical plant power generated throughout a 24 h period on 21 June and 21 December, while Table 2 presents an annual power output comparison.

Fig. 4 indicates no major difference in plant power production following the introduction of the new turbine inlet loss coefficient. Table 2 however, shows a slightly enhanced annual power output for the "Configuration B" plant. It follows that the inclusion of the new turbine inlet loss coefficient is responsible for a 0.6% rise in annual plant power production.

Table 2
Annual power output comparison, showing the influence of introducing a more realistic turbine inlet loss coefficient

Plant configuration	Annual power output [GWh]
Configuration A model (high loss)	776.4
Configuration B model (low loss)	780.7

4. Collector roof glass quality

Previous studies by Hedderwick (2001), Kröger and Buys (2001) and Pretorius et al. (2004) assumed a relatively poor quality glass as collector roof material. In terms of the current investigation, better quality glass implies a better transparency, thereby allowing more solar radiation transmittance. For partially transparent media, such as glass, a material constant known as the extinction coefficient partially determines the amount of radiation absorbed and subsequently transmitted by the medium. According to Duffie and Beckman (1991), the value of the extinction coefficient for glass varies from 32 m^{-1} for "greenish cast of edge" glass (having a somewhat greenish edge colour) to 4 m^{-1} for "water white" glass (having a whitish edge colour). With the motivating factor that better quality glass does not differ significantly in cost from the poorer quality glass previously used, it was decided to employ an improved glass collector roof with an extinction coefficient of $C_e = 4\ m^{-1}$.

4.1. Simulation and results

The "Configuration C" plant model is defined as equivalent to the "Configuration B" model, although including a better quality glass with an extinction

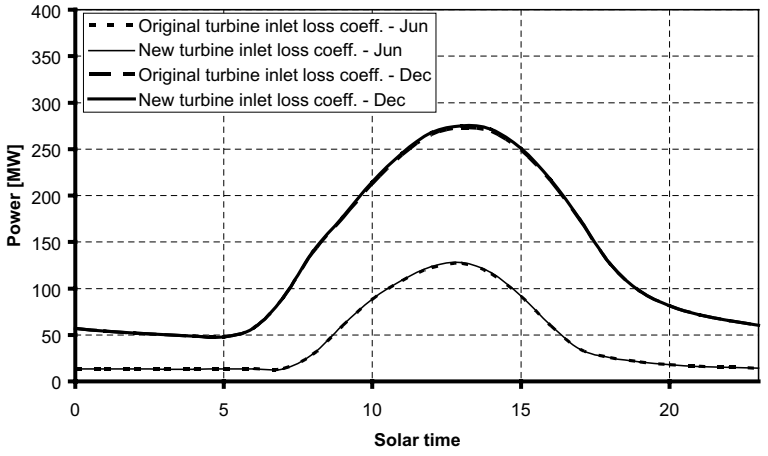

Fig. 4. Influence of the inclusion of a more realistic turbine inlet loss coefficient.

coefficient of $C_e = 4\ m^{-1}$. A simulation was conducted for the "Configuration C" model and compared to the results from the "Configuration B" model simulation, consequently evaluating the effect of the inclusion of a better quality glass roof.

Fig. 5 illustrates the maximum electrical plant power on 21 June and 21 December, while Table 3 compares the annual power output of the "Configuration B" and "Configuration C" plants.

When evaluating Fig. 5, it is clear that during the summer months the better quality glass causes a somewhat increased plant power output throughout the day, with a slightly higher peak value. The overall output during the colder months is also slightly higher, with the peak output marginally reduced. Another noticeable trend is that the model incorporating the poorer quality glass produces a higher output during winter mornings than the plant employing the better quality glass. This is due to the fact that the poorer quality glass is less transparent than the better quality glass. More energy is absorbed by the poorer glass in the mornings, resulting in a higher collector roof temperature. Conversely, the better glass allows more of the solar radiation to penetrate and strike the ground, causing a lower roof temperature than with poor quality glass. As a result, the temperature difference between the roof and the collector air is smaller when employing poor quality glass, while the value of h_{rh} is approximately similar for both plant configurations. The net result during cold mornings is that less heat is transferred from the collector air to the roof and less heat is lost to the environment when including a poorer quality glass roof.

Nevertheless, Table 3 substantiates the positive influence of a better quality glass on the annual power output of the solar chimney power plant, indicating an increase of approximately 3.4%.

Table 3
Annual power output comparison, illustrating the influence of including a better quality glass for the collector roof

Plant configuration	Annual power output [GWh]
Configuration B model (poor glass)	780.7
Configuration C model (good glass)	807.1

5. Various ground types

The previously mentioned studies by Hedderwick (2001), Kröger and Buys (2001) and Pretorius et al. (2004) employed Granite as the ground type for their solar chimney power plant simulations. However, many different ground types exist at locations around the world suitable for the construction of a solar chimney power plant. The following section evaluates the effect of two other ground types on the power production of a solar chimney plant. Although ground properties may vary, average values are selected from literature.

The Granite ground properties used by the abovementioned studies were selected from Holman (1992). Average properties for two other ground types, Limestone and Sandstone, are now also selected from the same text and listed in Table 4. It is clear that, according to the practically identical heat penetration coefficients ($b_p = \sqrt{\rho c_p k}$) of Limestone and Sandstone in Table 4, simulations corresponding to these two ground types should produce virtually similar results.

5.1. Simulation and results

The "Configuration D" plant model is defined as equivalent to the "Configuration C" model, but with Limestone employed as ground type instead of Granite.

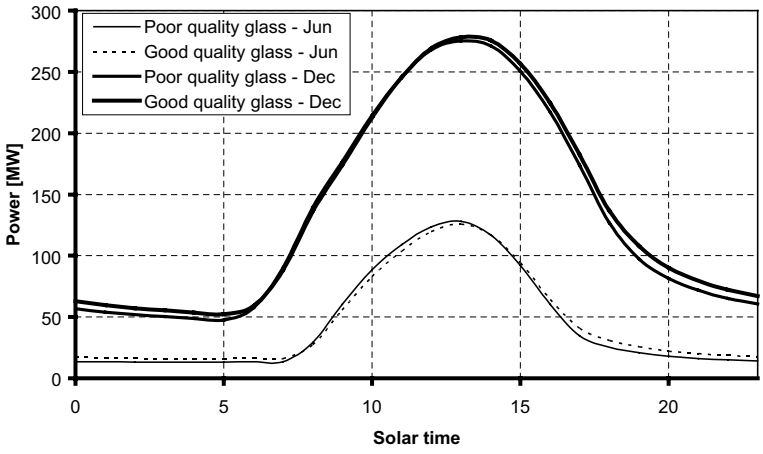

Fig. 5. Effect of the inclusion of a better quality glass for the collector roof.

Table 4
Average properties of Limestone and Sandstone according to Holman (1992)

Ground type	Density [kg/m^3]	Specific heat capacity [J/kg K]	Thermal conductivity [W/m K]	Heat penetration coefficient b_p [W s$^{1/2}$/K m^2]
Limestone	2500	900	1.26	1684
Sandstone	2160	710	1.83	1675
Granite	2640	820	1.73	1935

Similarly, the "Configuration E" plant model is defined as equivalent to the "Configuration C" model with Sandstone as ground type in place of Granite. In order to evaluate the effect that the respective Limestone and Sandstone soil types have on the power output of the solar chimney power plant, simulations were conducted for the "Configuration D" and "Configuration E" plant models and compared to the "Configuration C" plant simulation results.

The results shown in Fig. 6 indicate the maximum electrical power output for 21 June and 21 December for the various ground types investigated. Closer inspection of Fig. 6 reveals that the curves for the Limestone and Sandstone models are virtually indistinguishable, both for June and December. Thus there is no marked difference between the power outputs of a plant employing Limestone versus a plant employing Sandstone as its soil type, which confirms the assumption made earlier according to the virtually similar heat penetration coefficients of Limestone and Sandstone in Table 4. Furthermore, the plants employing Limestone and Sandstone indicate a lower power output during the night and greater power generation for most of the day, compared to the simulation model based on Granite.

Annually, Table 5 confirms the comparable results of the Limestone and Sandstone-based plants. These plants do not exceed the annual power output of the Granite-based ("Configuration C") solar chimney power plant significantly, showing only a 0.3% rise in annual output.

Table 5
Annual power output comparison for a solar chimney power plant employing various ground types

Plant configuration	Annual power output [GW h]
Configuration C model (Granite)	807.1
Configuration D model (Limestone)	809.6
Configuration E model (Sandstone)	809.7

6. Optimizing the collector roof shape and inlet height

Simulations were conducted by Pretorius et al. (2004) in order to determine the optimal collector roof shape and height, resulting in a maximum annual solar chimney power plant output. Specifically, simulations were performed using various roof shape exponents and inlet heights for a plant equivalent to the "Configuration A" plant (as specified in Appendix A of this paper). The

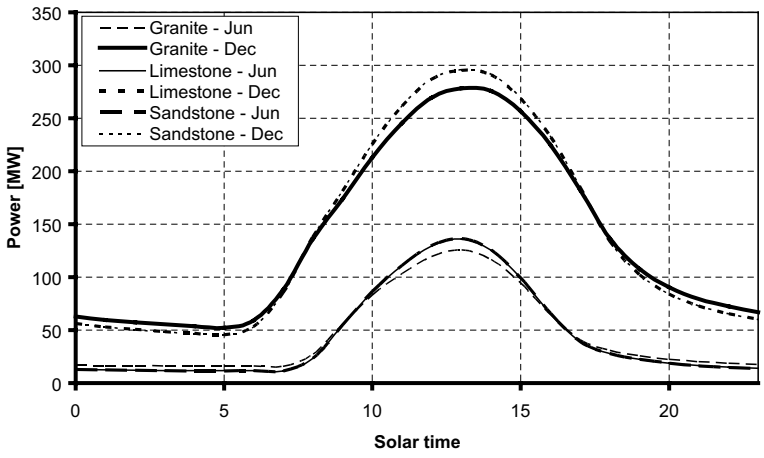

Fig. 6. The influence of various ground types on the daily power output of a solar chimney power plant.

above-mentioned plant model employed the original convective heat transfer equations as previously discussed. The simulation found that the plant produced a maximum annual power output with $b = 1$ and $H_2 = 3.3$ m (see Fig. 1).

The inclusion of the new convective heat transfer equation fundamentally changes the performance characteristics of the solar chimney power plant. It is therefore necessary to repeat the simulations performed by Pretorius et al. (2004) for various combinations of b and H_2 in order to determine a new optimal plant collector.

6.1. Simulation and results

Multiple simulations were performed for all combinations of three roof shape exponents and various collector roof inlet heights using the previously mentioned "Configuration C" plant as reference. The "Configuration C" plant model is based on the "Configuration A" model specified in Appendix A, however, including the new convective heat transfer correlation, the more realistic turbine inlet loss coefficient and good quality glass for the collector roof.

In order to provide a good basis for comparison, simulations were also performed for the "Configuration C" plant that incorporates the original convective heat transfer equations. This model incorporates the realistic turbine inlet loss coefficient and good quality collector roof glass. By drawing a comparison between the above-mentioned models, the effect of the inclusion of the new convective heat transfer correlation on the optimization of the plant is made clear. Thus, Fig. 7 draws an annual power output comparison for all combinations of three roof shape exponents and collector inlet heights for two versions of the "Configuration C" plant model, one incorporating the original and one including the new convective heat transfer correlation. Roof shape exponents no larger than one were employed in order to avoid flow separation under the collector roof.

When regarding Fig. 7, it is evident that the greatest power output is facilitated by the roof shape exponent $b = 1$, as found by Pretorius et al. (2004). This seems to be the only similarity to previous results. Previous findings by Pretorius et al. (2004) established a clear optimum collector inlet height for each b exponent value, as illustrated in Fig. 7 by the results of the model that incorporates the original heat transfer equations. This differs from current results, with the annual power output of the model employing the new convective heat transfer correlation reaching no maximum point for the inlet heights evaluated.

Previous results predicted higher plant power production with a collector inlet height of e.g. $H_2 = 3$ m than a plant with an inlet height of e.g. $H_2 = 6$ m. A lower collector inlet height means a smaller collector flow area, giving a higher collector airflow velocity. Previously, for these higher collector airflow velocities Eq. (3) predicted high h_{gh} values and somewhat lower h_{rh} values, resulting in significant energy extraction from the ground, small energy losses through the roof and ultimately high plant power generation. For lower collector air velocities, Eq. (3) predicted low h_{gh} and very low h_{rh} values, which caused a lower plant power output.

The introduction of Eq. (2) now leads to simulations estimating higher plant outputs for a plant using e.g. $H_2 = 6$ m than for plants employing e.g. $H_2 = 3$ m. The improved heat transfer correlation calculates high values

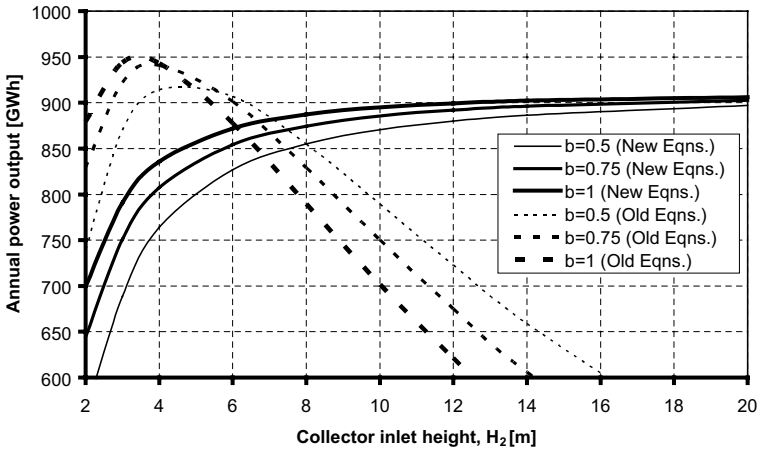

Fig. 7. Annual power output for various roof shapes and collector inlet heights for two versions of the "Configuration C" model, with one incorporating the original and the other the new convective heat transfer equation.

for h_{gh} and h_{rh} at low collector roof heights (therefore higher collector airflow velocities) and corresponding lower coefficient values at higher roof heights (therefore lower collector airflow velocities). With lower collector roofs, the high h_{gh} values imply good ground energy extraction. However, the high h_{rh} values also mean high energy losses through the collector roof to the environment. At higher collector roofs (giving lower airflow velocities), Eq. (2) still predicts good, although lower ground energy extraction while the energy losses through the roof also decrease. Current results therefore suggest that the higher the collector roof is the lower the airflow velocity becomes, giving lower heat losses through the roof and higher plant power production. Consequently, the plant model with the highest collector roof predicts the highest annual power output, as depicted in Fig. 7.

It should also be noted that at night, where Eq. (1) predicted a constant roof to ambient heat transfer coefficient of $h_{ra} = 5.7$ W/m^2 K, Eq. (2) now predicts lower h_{ra} values. Thus the convective heat flux from the collector roof to the environment at night is somewhat lower than previously calculated. This contributes to a lower heat loss to the ambient air and therefore slightly improves the plant output at night.

The optimal plant collector configuration may therefore be quite different to those suggested by previous optimal results. The optimal collector configuration will rather be found when employing plant power output, plant dimensions and construction costs as optimization constraints.

7. Conclusion

This paper critically evaluated the performance of a large scale solar chimney power plant. The effect of including a recently developed convective heat transfer equation, more realistic turbine inlet loss coefficient and better quality collector roof glass was investigated. The influence of various types of soil on the plant power output was established. The study concludes that the new heat transfer equation reduces the annual plant power output by 11.7%. The more realistic turbine inlet loss coefficient only accounts for a 0.6% rise in annual plant power production, while utilizing better quality glass increases the annual plant power output by 3.4%. Simulation models employing Limestone and Sandstone soil produce virtually similar results to the original model using Granite. The inclusion of the improved convective heat transfer equation fundamentally changes the performance characteristics of the solar chimney power plant. The resultant optimal solar chimney power plant collector height is not as predicted by Kröger and Buys (2001) or Pretorius et al. (2004).

Appendix A

For comparison purposes, a reference solar chimney power plant and typical operating environment is defined below (see Fig. 1). This model is referred to as the "Configuration A" plant.

Collector roof	
Emittance	$\epsilon_r = 0.87$
Perimeter height	$H_2 = 3.3$ m
Perimeter diameter	$d_2 = 7000$ m
Inside diameter	$d_3 = 400$ m
Inlet loss coefficient	$K_i = 1$
Roughness	$\varepsilon_r = 0$ m
Support diameter	$d_s = 0.15$ m
Support drag coefficient	$C_{sD} = 1$
Support tangential pitch	$P_t = 10$ m
Support radial pitch	$P_r = 10$ m
Extinction coefficient	$C_e = 32$ m^{-1}
Roof shape exponent	$b = 1$
Refractive index	$n_r = 1.526$
Thickness	$t_r = 0.005$ m
Ground	
Type	Granite
Emittance	$\epsilon_g = 0.9$
Absorptance	$\alpha_g = 0.9$
Density	$\rho_g = 2640$ kg/m^3
Specific heat capacity	$c_{pg} = 820$ J/kg K
Thermal conductivity	$k_g = 1.73$ W/m K
Roughness	$\varepsilon_g = 0.05$ m
Chimney	
Height	$H_c = 1500$ m
Inside diameter	$d_c = 160$ m
Bracing wheel (one) drag coefficient	$K_{bw} = 0.01$
Number of bracing wheels	$n_{bw} = 10$
Inside wall roughness	$\varepsilon_c = 0.002$ m
Turbine	
Turbo-generator efficiency	$\eta_{tg} = 80\%$
Inlet loss coefficient	$K_{turb,i} = 0.25$
Ambient conditions	
Atmospheric pressure	$p_a = 90000$ N/m^2
Wind speed	$v_w = 0$ m/s

References

Berdahl, P., Fromberg, R., 1982. The thermal radiance of clear skies. Solar Energy 29 (4), 299–314.

Bernardes, M.A., Dos, S., Voß, A., Weinrebe, G., 2003. Thermal and technical analyses of solar chimneys. Solar Energy 75 (6), 511–524.

Burger, M., 2004. Personal Communication. University of Stellenbosch, Stellenbosch, South Africa.

Duffie, J.A., Beckman, W.A., 1991. Solar Engineering of Thermal Processes. John Wiley and Sons, Inc., New York (Chapter 5).

Gannon, A.J., Von Backström, T.W., 2002. Controlling and maximizing solar chimney power output. In: Proceedings of the 1st International Conference on Heat Transfer, Fluid Mechanics and Thermodynamics, Kruger Park, South Africa.

Gannon, A.J., Von Backström, T.W., 2003. Solar chimney turbine performance. Journal of Solar Energy Engineering 125, 101–106.

Haaf, W., Friedrich, K., Mayr, G., Schlaich, J., 1983. Solar chimneys, part I: principle and construction of the pilot plant in Manzanares. International Journal of Solar Energy 2, 3–20.

Haaf, W., 1984. Solar chimneys, part II: preliminary test results from the Manzanares pilot plant. International Journal of Solar Energy 2, 141–161.

Hedderwick, R.A., 2001. Performance evaluation of a solar chimney power plant. Masters Thesis, University of Stellenbosch, Stellenbosch, South Africa.

Holman, J.P., 1992. Heat Transfer. McGraw-Hill, New York.

Kröger, D.G., Burger, M., 2004. Experimental convection heat transfer coefficient on a horizontal surface exposed to the natural environment. In: Proceedings of the ISES EuroSun2004 International Sonnenforum 1, Freiburg, Germany, pp. 422–430.

Kröger, D.G., Buys, J.D., 2001. Performance evaluation of a solar chimney power plant. ISES 2001 Solar World Congress, Adelaide, Australia.

McAdams, W.H., 1954. Heat Transmission. McGraw-Hill, New York.

Padki, M.M., Sherif, S.A., 1999. On a simple analytical model for solar chimneys. International Journal of Energy Research 23 (4), 345–349.

Pasumarthi, N., Sherif, S.A., 1998a. Experimental and theoretical performance of a demonstration solar chimney model—part I: mathematical model development. International Journal of Energy Research 22 (3), 277–288.

Pasumarthi, N., Sherif, S.A., 1998b. Experimental and theoretical performance of a demonstration solar chimney model—part II: experimental and theoretical results and economic analysis. International Journal of Energy Research 22 (5), 443–461.

Pretorius, J.P., Kröger, D.G., Buys, J.D., Von Backström, T.W., 2004. Solar tower power plant performance characteristics. In: Proceedings of the ISES EuroSun2004 International Sonnenforum 1, Freiburg, Germany, pp. 870–879.

Schlaich, J., 1994. The Solar Chimney: Electricity from the Sun. Deutsche Verlags-Anstalt, Stuttgart.

Von Backström, T.W., Kirstein, C.F., Pillay, L.A., 2003. The Influence of some secondary effects on solar chimney power plant performance. In: ISES 2003 Solar World Congress, Göteborg, Sweden.

Yan, M.Q., Sherif, S.A., Kridli, G.T., Lee, S.S., Padki, M.M., 1991. Thermo-fluid analysis of solar chimneys. In: Morrow, T.B., Marshall, L.R., Sherif, S.A. (Eds.), Industrial Applications of Fluid Mechanics-1991, FED, vol. 132. The American Society of Mechanical Engineers, New York, pp. 125–130 (Book #H00720).